Interactions of metronidazole and chloramphenicol with myoglobin: Crystal structure of a Mb-acetamide product

Samantha M. Powell[a,b,*], Kiana Y. Prather[a,c], Nancy Nguyen[a,c], Leonard M. Thomas[a], George B. Richter-Addo[a,*]

[a] *Price Family Foundation Institute of Structural Biology, Stephenson Life Sciences Research Center, and Department of Chemistry and Biochemistry, University of Oklahoma, 101 Stephenson Parkway, Norman, OK, U.S.A. 73019*

[b] *Biological Sciences Division, Pacific Northwest National Laboratory, 902 Batelle Blvd, Richland, WA, U.S.A. 99352*

[c] *University of Oklahoma College of Medicine, 800 Stanton L. Young Blvd, Oklahoma City, OK 73117*

Received date:

A contribution to the Jonathan Sessler special issue

ABSTRACT: Nitroorganics present a general concern for a safe environment due to their health hazards. However, some nitroorganics such as metronidazole (Mtz) and chloramphenicol (CAM) also possess medicinal value. Mtz and CAM can undergo reductive bioactivation presumably via their nitroso derivatives. We show, using UV-vis spectroscopy, that sperm whale myoglobin (swMb) and its distal pocket mutants retaining H-bonding capacity react with Mtz in the presence of dithionite to generate products with spectra suggestive of the Fe-bound nitroso (Fe–RNO; λ_{max} ~420 nm) forms. We have crystallized and solved the X-ray crystal structure of an H64Q swMb-acetamide compound to 1.76 Å resolution; formation of this compound results from the serendipitous crystallographic trapping, by the heme center, of acetamide from the reductive decomposition of Mtz. Only one of the swMb proteins, namely H64Q swMb with a relatively flexible Gln64 residue, reacted with CAM presumably due to the bulky nature of CAM that generally may restrict its access to the heme site.

* Correspondence to:

Samantha M. Powell, Biological Sciences Division, Pacific Northwest National Laboratory, Richland, WA, U.S.A. 99352. Tel: 509-375-6343. Email: samantha.powell@pnnl.gov

George B. Richter-Addo, Department of Chemistry and Biochemistry, University of Oklahoma, Norman, OK, U.S.A. 73019. Fax: 405-325-6111. Email: grichteraddo@ou.edu

KEYWORDS: Heme, myoglobin, metronidazole, chloramphenicol, X-ray structure, nitroso, acetamide

INTRODUCTION

Nitrooorganics including nitroaromatics pose significant threats to a healthy environment, as several members of this class are toxic, carcinogenic, and/or mutagenic [1-3]. Metalloporphyrins aid in the metabolism of some nitro-containing drugs and organics under reducing conditions (reviewed in [4,5]). The reactions generally involve conversion of the nitroorganic functionalities under reducing conditions to the nitroso forms (eq 1) that may bind directly to the heme sites (products with λ_{max} ~420 nm) as shown by us and others [6-10].

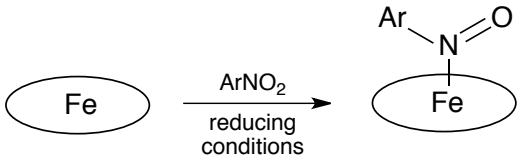

(1)

Metronidazole (Mtz) and chloramphenicol (CAM) are two widely prescribed drugs used for the treatment of bacterial infections. Sketches of their chemical structures are shown in Fig. 1.

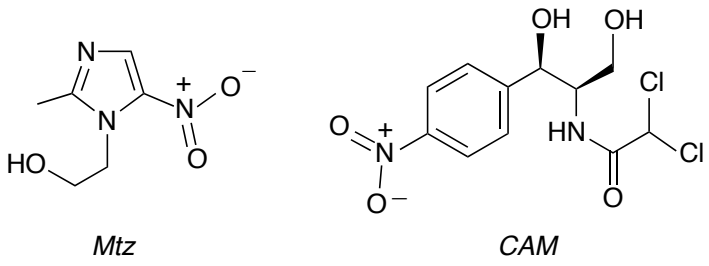

Fig. 1. Chemical structures of metronidazole (Mtz) and chloramphenicol (CAM).

Mtz is used in the treatment of *Clostridioides difficile* infections in the gut and the oral cavity, and is typically metabolized by the bacterial nitroreductase enzymes [11-13]. CAM is a much larger molecule that also contains a nitroorganic functionality, and is now only rarely used when other antibiotic treatments for serious infections are not effective [14]. The nitroso derivative of CAM is presumed to be one of the bioactive intermediates under reducing conditions, although its role in toxicity remains unclear [15,16].

We are interested in determining if the nitroso derivatives of Mtz and CAM are capable of binding to the Fe center of heme proteins. We thus pursued their reactions with the prototypical protein myoglobin, in particular the wild-type sperm whale Mb protein and selected distal pocket mutants that vary in H-bonding capacity to bound ligands. In this paper, we report our UV-vis spectral findings for these reactions, and also report the X-ray crystal structure of an unexpected, but important first member of the heme protein-acetamide family.

MATERIALS AND METHODS

The wild type and mutant sperm whale Mbs were obtained as previously described [17-19]. Metronidazole (Mtz; Fluka) and chloramphenicol (CAM; Sigma) were purchased from commercial suppliers and used as received.

UV-vis spectroscopy

UV-vis spectroscopy was used to monitor the reactions of ferric swMb^{III}–H_2O (wt and mutants) with Mtz and CAM. An initial reading was taken of the starting ferric Mb^{III}–H_2O (5 μL of 20 mg/mL) in 2.5 mL of 0.1 M sodium phosphate buffer at pH 7.4. Sodium dithionite (5 μL of a 1 M solution) was added to the cuvette to fully reduce the protein to ferrous deoxyMb^{II}, and a reading was taken. An aliquot of the substrate (10–15 μL; 50 mg/mL CAM or 20 mM Mtz) was then added to the cuvette. Readings were taken at different time points during the course of the reaction to monitor its progress.

Crystallization

The co-crystallization method was utilized to obtain crystals from the reaction of H64Q swMb with Mtz. Ferric H64Q swMb^{III}–H_2O (75 μL of a 20 mg/mL in 0.1 M sodium phosphate buffer at pH 7.4) was mixed with a few grains of solid Mtz and allowed to react for 15 min. A small of amount of solid sodium dithionite was then added to the mixture. Completion of the reaction was confirmed using UV-vis spectroscopy. Crystals were grown using the hanging drop vapor diffusion method as described by Phillips et al [20]. The wells contained 2.60 M ammonium sulfate, 100 mM Tris-HCl, 1 mM EDTA, pH 7.4, and the drops contained a 1:1 ratio of protein-reaction to well solution. The drops were seeded with crushed ferric H64A swMb^{III}–H_2O crystals after an equilibration period of 6 h. Crystals started forming after ~3 days, and

suitably-sized crystals were harvested after 17 days using cryoloops and were frozen in liquid nitrogen prior to data collection.

X-ray data collection

The diffraction data were collected at the University of Oklahoma Macromolecular Crystallography Lab (OU MCL) using a home source Rigaku MicroMax 007HF microfocus X-ray generator coupled to a PILATUS 200K detector. The data was collected at 100 K with Cu Kα radiation (λ = 1.54178 Å) from the generator operated at 40 kV/30 mA.

Data processing, structure solution and refinement

The X-ray diffraction data were processed using *HKL3000* and the resulting *sca* files were converted to *mtz* using *Scalepack2mtz* in the CCP4 program suite [21]. *PHASER MR* (CCP4) [22] was used to determine the initial phases. The model used for molecular replacement was wt swMb (ferric Mb^{III}–H_2O) at 1.5 Å resolution (PDB ID: 2MBW) with the heme, water molecules and ligands removed from the structure. Refinements were performed using *Refmac5* (CCP4) [23] and *phenix.refine* [24]. Models were rebuilt using *COOT* [25] and validated using *MolProbity* [26] to check for unusual residue conformations and contacts.

The figures for each structure were generated using *Pymol* [27]. $2F_o–F_c$ electron density maps were calculated by *Fast Fourier Transform* (FFT; CCP4) [28]. $F_o–F_c$ electron density maps were generated by first deleting all ligands from the final *pdb* file of each structure. This *pdb* file was used to create a new F_c *mtz* file using *SFall* (CCP4). The F_c *mtz* file was used to generate the $F_o–F_c$ electron density map using *FFT*. The resulting *FFT map* files were converted to *ccp4* files and displayed in *Pymol*.

Ten initial cycles of restrained refinement were run with *Refmac5*, and the *R* factor decreased from 0.361 to 0.276. Ligands and water were added to the model based on the $F_o–F_c$ electron density maps in the subsequent refinement cycles. Two sulfate anions, two glycerol molecules and one acetamide (ligand id: ACM) were added to the model. The *N*-terminal Met and the *C*-terminal residues Q152 and G153 were omitted due to lack of electron density. Two conformations for the sidechains Val68 and Lys133 were modeled with 50% occupancy each. The final *R* factor and R_{free} were 0.204 and 0.221, respectively. The structure has been deposited with the Protein Data Bank with access code 8FB0.

RESULTS AND DISCUSSION

UV-vis spectral monitoring

UV-vis spectral monitoring of the reactions of the Mb proteins with Mtz and CAM revealed that, in selected cases, products formed that were suggestive of the target ferrous nitroso Mb^{II}–RNO derivatives being generated. An initial spectral reading was taken of ferric wild-type or mutant $swMb^{III}$–H_2O (λ_{max} ~409 nm) as the starting point. Dithionite was added to reduce the protein to its ferrous $deoxyMb^{II}$ form (λ_{max} ~433 nm) [29,30] and as a result, shifts in the Soret band from ~409 to ~433 nm. Similar spectra were observed for the mutant proteins (Fig. 2).

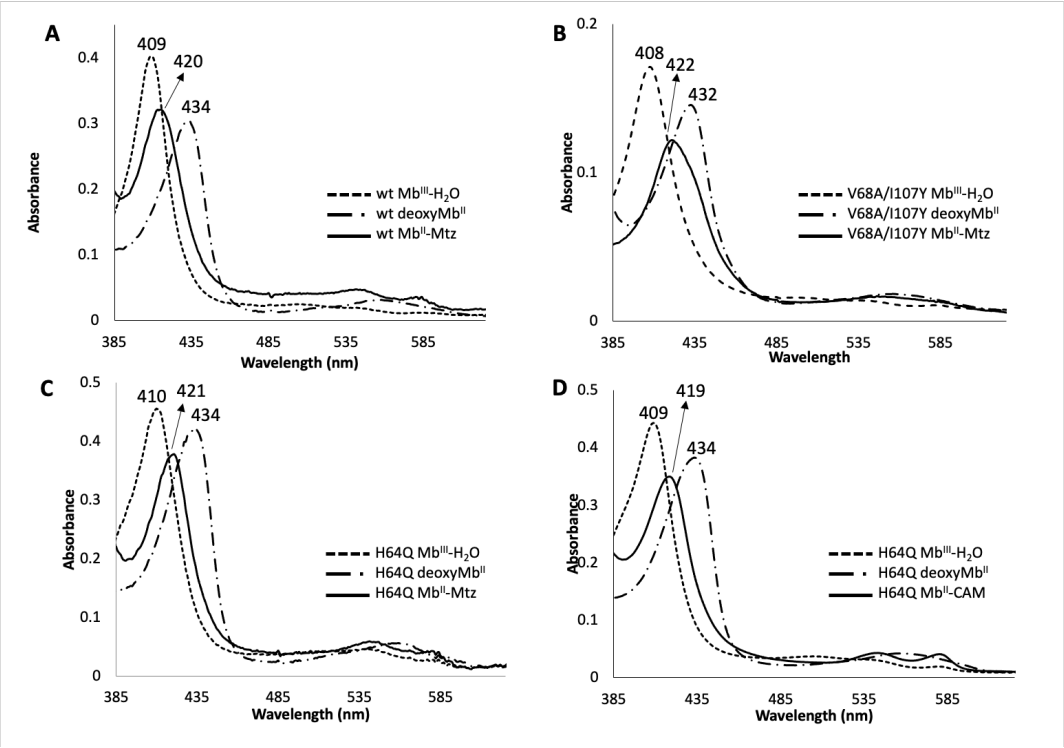

Fig. 2. UV-vis spectral changes during the reactions of (A) wt Mb with Mtz, (B) V68A/I107Y Mb with Mtz, (C) H64Q Mb with Mtz, and (D) H64Q Mb with CAM. Conditions: 0.1 M phosphate buffer, pH 7.4, [protein] = 2.0 μM, [dithionite] = 2 mM, [Mtz] = 350 μM or [CAM] = 600 μM.

Mtz or CAM was then added to the cuvette containing the reduced protein. In the case of ferrous $deoxyMb^{II}$ in its reaction with Mtz, the peak in the Soret band shifted from λ_{max} 434 nm for the reduced protein to 420 nm (Fig. 2A) and the reaction was complete after ~20 min. Similar

shifts were seen in the Soret bands for both ferrous V68A/I107Y (432 to 422 nm) and H64Q Mb^{II} (434 to 421 nm) in their reactions with Mtz (Figs. 2B-C). Reaction of the H64Q Mb mutant with Mtz was complete after ~5 min, but the reaction with the V68A/I107Y Mb mutant took ~75 min to reach completion.

Interestingly, ferric H64Q Mb^{III}–H_2O was the only form of swMb that reacted with CAM, resulting in shifts in the Soret band from 434 to 419 nm (Fig. 2D); this reaction was complete after ~10 min. The data in Table 1 summarizes these UV-vis spectral observations. The spectra are not shown for the reactions of the other reduced Mb proteins with CAM that did not occur, as the spectra remained the same as those of the reduced deoxyMb^{II} species.

Table 1. Summary of the interaction of the reduced swMbs with Mtz and CAM showing times to completion.

Ligand	wtMb	H64A	H64Q	H64V	V68A/I107Y
Mtz	420 nm at 20 min	No rxn	421 at 5 min	No rxn	422 at 75 min
CAM	No rxn	No rxn	419 nm at 10 min	No rxn	No rxn

Analysis of the reactions of the reduced swMbs with Mtz and CAM

Our results summarized in Table 1 suggest that a distal pocket H-bonding residue is necessary for the product formation from the reaction of both CAM and Mtz with the reduced Mb^{II} centers, since neither CAM nor Mtz reacted with the H64A or H64V mutants that do not contain such distal pocket H-bonding residues. Mtz did react with ferric wt, H64Q and V68A/I107Y Mb^{II} proteins, suggesting that Mtz does not have a preference for a particular amino acid at position 64 but does require a H-bonding residue in this location.

Interestingly, although CAM reacted with the reduced H64Q Mb mutant to generate a product with λ_{max} of 419 nm assigned to the nitroso derivative, we did not observe reactions with either the wt or V68A/I107Y Mb proteins although the latter also contain distal pocket H-bonding residues. These results suggest that CAM has a preference for Gln over His in position 64, probably due to the fact that CAM is a larger substrate than Mtz, and likely requires a more flexible amino acid like Gln in position 64 to allow CAM to enter the pocket.

Crystallography: X-ray crystal structure of H64Q swMb with acetamide

We pursued multiple crystallization efforts in attempts to obtain diffraction-quality crystals for the target ferrous Mb^{II}–RNO derivatives (i.e., the products with λ_{max} ~420 nm in Fig. 2) but were not successful. However, one of our attempts led to the determination of a crystal structure of a heme-acetamide product that coincidentally has structural biology relevance in its own right.

Our attempt to crystallize the product from the reactions of ferric H64Q $swMb^{III}$–H_2O with Mtz in the presence of dithionite as the reducing agent yielded suitable crystals of a product whose X-ray crystal structure was solved to 1.76 Å resolution; data collection and refinement statistics are collected in Table 2.

Table 2. Data collection and refinement statistics

Data collection[a]		**Refinement statistics**	
Space group	*P6*	No. of protein atoms	1262
Cell dimensions: *a*, *b*, *c* (Å); α, *β*, *γ* (°)	90.29, 90.29, 45.26 90.00, 90.00, 120.00	*R* factor[c]	0.150
Resolution (Å)	45.26-1.76	R_{free}[d]	0.0.178
I/σ[I]	24.79 (9.06)	RMSD Bond length (Å)	0.019
No. of observed reflns	22224	RMSD Bond angles (°)	1.99
No. of unique reflns	21041 (2046)	Overall Mean B Factor (Å^3)	14.43
Multiplicity	1.8 (1.4)	Ramachandran plot (%)[e]	
Completeness (%)	99.8 (98.3)	most favored residues	98.01
R_{merge}[b]	0.024 (0.058)	outliers	0.00
$CC_{1/2}$	0.999		

(a) Values in parentheses correspond to the highest resolution shells. (b) $R_{merge} = \Sigma|I - \langle I \rangle|/\Sigma(I)$, where I is the individual intensity observation and $\langle I \rangle$ is the mean of all measurements of I. (c) $R = \Sigma||F_o|-|F_c||/\Sigma|F_o|$, where F_o and F_c are the observed and calculated structure factors, respectively. (d) R_{free} was calculated by using 5% of the randomly selected diffraction data, which were excluded from the refinement. (e) As calculated using *MolProbity*.

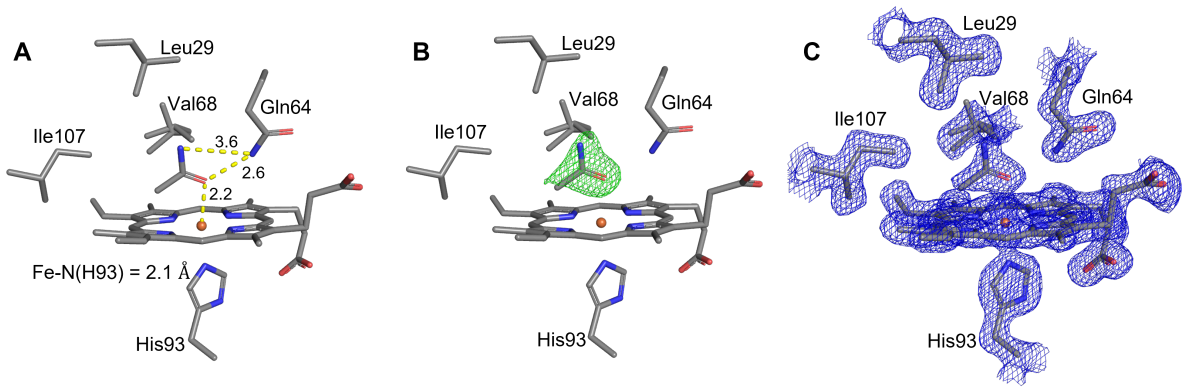

Fig. 3. X-ray crystal structure of ferrous H64Q swMb–ACM showing only the active site. (A) Final model of the active site showing the closest interactions of the ACM ligand with the Fe center and Gln64 residue. (B) The F_o–F_c omit map (contoured at 1.5 σ) showing the presence of electron-density assigned to ACM. (C) The corresponding $2F_o$–F_c map (contoured at 1.0 σ).

The crystal structure of this Mb product, focusing on the heme active site, is shown in Fig. 3. Curiously, the new electron density in the F_o–F_c omit maps did not match that of an Mtz-bound species (Figs. 3B-C). Instead, the new electron density at the heme site best matched that of acetamide ($CH_3C(=O)NH_2$; ACM) which was modeled in its *O*-bound form as determined in non-protein models [31,32]. The Fe–O(ACM) distance is 2.2 Å and is close to the analogous distance of 2.091(1) Å determined in the six-coordinate bis-acetamide heme model $[(TPP)Fe(O=C(NH_2)CH_3)_2]ClO_4$ complex reported earlier [31]. The ACM ligand engages in a H-bond interaction with the distal pocket Gln64 residue with a heteroatom (ACM)O···H_2N(Gln) bond distance of 2.6 Å.

Importantly, acetamides are known to interact with heme proteins. For example, allyl isopropyl acetamide depletes cytoplasmic heme via degradation of the cytochrome P450 heme [33,34]. It is thus surprising that not much is currently known about the structural consequences of acetamide binding to heme. It is also interesting to note that a dichloroacetamide product arises from the Fe-mediated decomposition of chloramphenicol (CAM)[35]. To the best of our knowledge, our Mb-acetamide structure described above in Fig. 3 is the first reported X-ray crystal structure of a heme protein with a bound acetamide ligand.

Likely origin of the acetamide fragment in the X-ray crystal structure

Based on the UV-vis studies above (Fig. 2C) describing the reaction of ferric H64Q Mb^{III}–H_2O with Mtz in the presence of the reducing agent dithionite, we expected to find Mtz bound to the Fe center in the crystal structure. However, we found that it was acetamide (ACM) that was bound instead. Notably, the reaction between the Mb protein and Mtz was carried out in the presence of dithionite that does not seem to affect the integrity of the targeted Mb-RNO product over short time periods.

It is known that sodium dithionite by itself can reductively activate Mtz, eventually leading to ring fission generating hydroxyethyl oxamic acid and ACM (Fig. 4) [11].

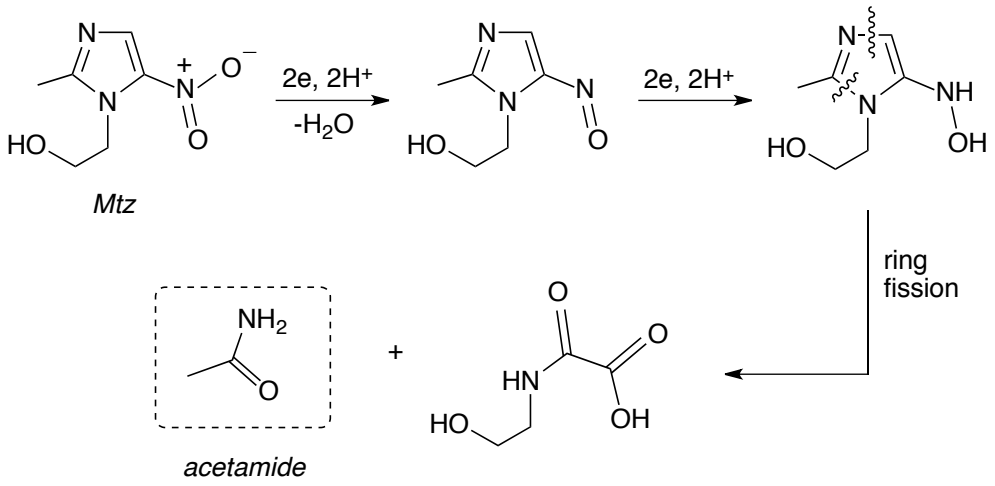

Fig. 4. Reductive activation of Mtz via the nitroso and hydroxylamino derivatives en route to acetamide (ACM) formation (adapted from ref [11]).

It is thus likely that, during the extended time period the complex remained in the crystallization well prior to crystal harvesting (~3 weeks) a portion of the Mtz reagent was cleaved by dithionite to generate ACM, and the crystals obtained were those from the contributing [Mb+ACM] reaction.

CONCLUSIONS

We have demonstrated that the antibiotic Mtz reacts with wild-type and mutant (H64Q and V68A/I107Y) myoglobin under reducing conditions to generate compounds with spectra

suggestive of nitroso (Fe–RNO; λ_{max} ~420 nm) formation in solution as determined by UV-vis spectroscopy. The lack of observed reactivity with the H64A and H64V mutants suggests that the presence of a distal-pocket H-bonding residue is required for the success of the reaction under our experimental conditions. Similar reactivity with CAM was only observed for the H64Q mutant protein that contains a relatively flexible Gln residue at position 64, consistent with the relatively larger size of CAM versus Mtz for entry into the distal pocket. Our attempts to crystallize one such product resulted in our X-ray structural determination of the first heme protein-acetamide complex, namely that of H64Q swMb-acetamide. Our results thus provide the first X-ray structural confirmation that acetamide can indeed serve as a ligand that binds directly to the Fe center in heme proteins. Given that acetamide is a common chemical in use in the solvent and plastics industries, we now have an opportunity to utilize this Mb-acetamide structure as a framework for further studies in this area of heme-acetamide interactions.

Acknowledgements

This material is based upon work supported by (while GBR-A was serving at) the U.S. National Science Foundation (NSF; CHE-2154603 and CHE-1900181). Any opinion, findings, and conclusions or recommendations expressed in this material are those of the authors and do not necessarily reflect the views of the NSF. This paper reports data obtained in the University of Oklahoma Macromolecular Crystallography Laboratory which is supported, in part, by an Institutional Development Award (IDeA) from the National Institute of General Medical Sciences of the National Institutes of Health under grant number P20GM103640, and by a Major Research Instrumentation award from the National Science Foundation under award number 092269.

REFERENCES

1. Roldan M, Perez-Reinado E, Castillo F and Moreno-Vivian C. *FEMS Microbiol. Rev.* 2008; **32**: 474-500.
2. O'Brien PJ, Wong WC, Silva J and Khan S. *Xenobiotica* 1990; **20**: 945-955.
3. Kovacic P and Somanathan R. *J. Appl. Toxicol.* 2014; **34**: 810-824.
4. Lee J, Chen L, West AH and Richter-Addo GB. *Chem. Rev.* 2002; **102**: 1019-1065.
5. Xu N and Richter-Addo GB. *Prog. Inorg. Chem.* 2014; **59**: 381-445.

6. Mansuy D, Gans P, Chottard J-C and Bartoli J-F. *Eur. J. Biochem.* 1977; **76**: 607-615.
7. Mansuy D, Chottard JC and Chottard G. *Eur. J. Biochem.* 1977; **76**: 617-623.
8. Mansuy D, Beaune P, Cresteil T, Bacot C, Chottard J-C and Gans P. *Eur. J. Biochem.* 1978; **86**: 573-579.
9. Copeland DM, West AH and Richter-Addo GB. *Proteins: Struct., Func., Genet.* 2003; **53**: 182-192.
10. Yi J, Ye G, Thomas LM and Richter-Addo GB. *Chem. Commun.* 2013; **49**: 11179-11181.
11. Dingsong SA and Hunter N. *J. Antimicrob. Chemother.* 2018; **73**: 265-279.
12. McFarland LV. *Expert Opin. Invest. Drugs* 2016; **25**: 541-555.
13. Leffler DA and Lamont JT. *Gastroenterology* 2009; **136**: 1899-1912.
14. Yunis AA. *Ann. Rev. Pharmacol. Toxicol.* 1988; **28**: 83-100.
15. Eyer P, Lierheimer E and Schneller M. *Biochem. Pharmacol.* 1984; **33**: 2299-2308.
16. Abou-Khalil S, Abou-Khalil WH and Yunis AA. *Biochem. Pharmacol.* 1980; **29**: 2605-2609.
17. Springer BA and Sligar SG. *Proc. Natl. Acad. Sci. USA* 1987; **84**: 8961-8965.
18. Wang B, Shi YL, Tejero J, Powell SM, Thomas LM, Gladwin MT, Shiva S, Zhang Y and Richter-Addo GB. *Biochemistry* 2018; **57**: 4788-4802.
19. Wang B, Thomas LM and Richter-Addo GB. *J. Inorg. Biochem.* 2016; **164**: 1-4.
20. Phillips GN, Arduini RM, Springer BA and Sligar SG. *Proteins: Struc., Func., Genet.* 1990; **7**: 358-365.
21. Winn MD, Ballard CC, Cowtan KD, Dodson EJ, Emsley P, Evans PR, Keegan RM, Krissinel EB, Leslie AGW, McCoy A, McNicholas SJ, Murshudov GN, Pannu NS, Potterton EA, Powell HR, Read RJ, Vagin A and Wilson KS. *Acta Cryst.* 2011; **D67**: 235-242.
22. McCoy AJ, Grosse-Kunstleve RW, Adams PD, Winn MD, Storoni LC and Read RJ. *J. Appl. Cryst.* 2007; **40**: 658-674.
23. Murshudov GN, Vagin AA and Dodson EJ. *Acta Cryst.* 1997; **D53**: 240-255.
24. Afonine PV, Grosse-Kunstieve, RW, Echols N, Headd JJ, Moriaty NW, Mustyakimov M, Terwilliger TC, Urzhumstev A, Zwart PH and Adams PD. *Acta Cryst. Section D* 2012; **D68**: 352-367.
25. Emsley P and Cowtan K. *Acta Cryst.* 2004; **D60**: 2126-2132.
26. Chen VB, Arendall WB, Headd JJ, Keedy DA, Immormino RM, Kapral GJ, Murray LW, Richardson JS and Richardson DC. *Acta Cryst.* 2010; **D66**: 12-21.
27. *PYMOL* 2022. Schrödinger-LLC; www.pymol.org.
28. Read RJ and Schierbeek AJ. *J. Appl. Cryst.* 1988; **21**: 490-495.
29. Cox RP and Hollaway MR. *Eur. J. Biochem.* 1977; **74**: 575-587.
30. Yi J, Heinecke J, Tan H, Ford PC and Richter-Addo GB. *J. Am. Chem. Soc.* 2009; **131**: 18119-18128. .
31. Xu N, Guan Y, Nguyen N, Lingafelt C, Powell DR and Richter-Addo GB. *J. Inorg. Biochem.* 2019; **194**: 160-169.

32. Xu N, Bevak AW, Armstrong BR and Powell DR. *Polyhedron* 2017; **127**: 432-437.
33. Fagard R and Guguenguillouzo C. *Biochem. Biophys. Res. Commun.* 1983; **114**: 612-619.
34. Matteis FD. *Biochem. J.* 1971; **124**: 767-777.
35. Chu WH, Ding SK, Bond T, Gao NY, Yin DQ, Xu B and Cao ZQ. *Water Res.* 2016; **104**: 254-261.

Graphical Abstract

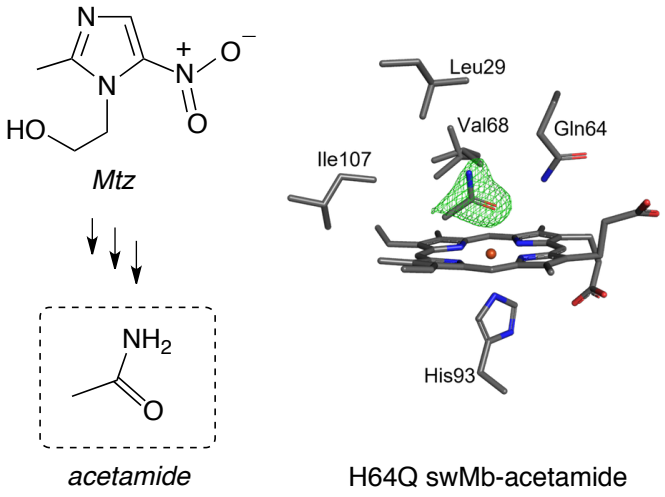

The heme protein myoglobin (Mb) and its distal pocket mutants H64Q and V68A/I107Y react with the antibiotic metronidazole (Mtz) under reducing conditions to form products assigned as the nitroso (Fe–RNO; λ_{max} ~420 nm) derivatives. Attempted crystallization of the H64Q product resulted in the first structural determination of a heme protein-acetamide complex.